CANCER BIOLOGY & THERAPY
2018, VOL. 19, NO. 1, 63–75
https://doi.org/10.1080/15384047.2017.1385675

Taylor & Francis
Taylor & Francis Group

RESEARCH PAPER

Some chemotherapeutics-treated colon cancer cells display a specific phenotype being a combination of stem-like and senescent cell features

H. Was[a,d], J. Czarnecka[a], A. Kominek[b], K. Barszcz[a], T. Bernas[c], K. Piwocka[b], and B. Kaminska[a]

[a]Laboratory of Molecular Neurobiology, Nencki Institute of Experimental Biology, Polish Academy of Sciences, Pasteur 3 street, Warsaw, Poland; [b]Laboratory of Cytometry, Nencki Institute of Experimental Biology, Polish Academy of Sciences, Pasteur 3 street, Warsaw, Poland; [c]Laboratory of Imaging Tissue Structure and Function, Nencki Institute of Experimental Biology, Polish Academy of Sciences, Pasteur 3 street, Warsaw, Poland; [d]Laboratory of Molecular Oncology, Military Institute of Medicine, Szaserów 128 street, Warsaw, Poland

ABSTRACT

Colorectal cancer (CRC) is the second leading cause of death among cancer patients in the Northern countries. CRC can reappear a long time after treatment. Recent clinical studies demonstrated that, in response to chemotherapy, cancer cells may undergo stress-induced premature senescence (SIPS), which typically results in growth arrest. Nonetheless, these senescent cells were reported to divide in an atypical manner and thus contribute to cancer re-growth. Therefore, we examined if SIPS escape may follow treatment with chemotherapeutics used clinically: 5-fluorouracil (5-FU), oxaliplatin (OXA) and irinotecan (IRINO).

To mimic the therapeutic regimes we exposed human colon cancer HCT116 and SW480 cells to repeated cycles of drug treatment. The cells treated with 5-FU or IRINO exhibited several hallmarks of SIPS: growth arrest, increased size and granularity, polyploidization, augmented activity of the SA-β-galactosidase, accumulation of P21 and CYCLIN D1 proteins, and the senescence-associated secretory phenotype. Moreover, re-population of the cancer cell cultures was delayed upon treatment with the senescence-inducing agents. At the same time, we detected a subpopulation of senescent colon cancer cells with features of stemness: elevated NANOG expression, exclusion of Hoechst 33342 (typical for side population) and increased CD24 expression. Additionally, rare, polyploid cells exhibited blastocyst-like morphology and produced progeny. In parallel, majority of chemotherapeutics-treated cells underwent mesenchymal to epithelial transition, as the percentage of CD44-positve cells was reduced, and levels of E-cadherin (epithelial marker) were elevated.

Our study demonstrates that a subpopulation of chemotherapeutics-treated colon cancer cells display a specific phenotype being a combination of stem-like and senescent cell features. This may contribute to their resistance to chemotherapy and their ability to re-grow cancer after completion of therapeutic intervention.

ARTICLE HISTORY
Received 7 December 2016
Revised 6 September 2017
Accepted 24 September 2017

KEYWORDS
cancer stem cells; chemotherapy; colon cancer; doxorubicin; irinotecan; oxaliplatin; senescence; 5-fluorouracil; angiogenesis; cancer Biology; cell Cycle control; molecular Therapy

Introduction

Colorectal cancer (CRC) is the second leading cause of death among cancer patients in the Northern countries.[1] Despite considerable improvements in the treatment of this disease with new therapeutic agents, the mortality rate is still significant.[2] Several combination of chemotherapy protocols are used for the initial treatment of metastatic colorectal cancer (mCRC) comprising at least two of the following drugs: 5-fluorouracil, oxaliplatin and irinotecan.[3,4] The antimetabolite 5-fluorouracil (5-FU) inhibits a thymidylate synthase, leading to depletion of 2′-deoxythymidine 5′-triphosphate – dTTP[5] and causing DNA damage during S phase.[6,7] Oxaliplatin, a third-generation platinum-derived chemotherapy agent, displays a wide spectrum of *in vitro* cytotoxic and *in vivo* antitumor activities. The mechanism of oxaliplatin toxicity includes alkylation of DNA.[8] Irinotecan, an inhibitor of topoisomerase I, induces formation of DNA double-strand breaks[9], activation of proteins involved in DNA damage checkpoint response (including ATM kinase) and consequently cell cycle arrest.[10,11] Combination of 5-FU with oxaliplatin and irinotecan increases patient response rates and prolongs progression-free survival.[12,13]

Notwithstanding advances in therapy, only 10% of metastatic CRC patients survive at least five years. Moreover, CRC can reappear at later times, even if the cancer tissue was entirely removed during the initial treatment.[14] Along with intrinsic drug resistance, tumor heterogeneity and clonal evolution, the stress-induced premature senescence (SIPS) is one of mechanisms of the drug resistance.[15–17] SIPS is an acute and short term effect, which is not dependent on telomere shortening. It may be triggered by oxidative stress or DNA damage, leading to irreversible growth arrest.[18] Recently, accumulation of senescent cancer cells has been linked to reduced survival of patients subjected to anticancer treatment.[15] This effect could be related to remodeling of tumor environment, mediated by the senescence associated secretory phenotype (SASP)[19] and/ or atypical division of senescent cells, called neosis.[20] Moreover, some

CONTACT H. Was hwas@wim.mil.pl Laboratory of Molecular Oncology, Military Institute of Medicine, Szaserów 128 street, 04-141 Warsaw, Poland.
Supplemental data for this article can be accessed on the publisher's website.

studies demonstrated that senescent cells may display a stem cell features.[21–27] The cancer stem cell (CSC) model of cancer origin suggests that only a small subset of cancer cells is responsible for sustaining tumorigenesis. CSCs exhibit the stem cell properties of self-renewal and an ability to differentiate into various lineages.[28] The presence of cancer stem cells (CSC) in haematopoietic malignancies and solid tumors, including CRC, has been extensively documented.[29–31] The CSC hypothesis explains resistance to chemotherapy and tumor recurrence, since quiescent or slow cycling CSCs may survive therapeutic intervention and produce a relapse.[28]

Here, we demonstrate that colon cancer HCT116 and SW480 cells undergo senescence in long term cultures and some of them acquire several features of stem cells following the treatment with 5-FU or IRINO. Additionally, we observed that rare, polyploid cells demonstrate blastocyst-like morphology and may produce progeny. Altogether, our data provide a new evidence that a senescent cancer cell might be considered as a new type of a tumor-initiating cell, which shows a mixed phenotype combining stem-like and differentiated cell features.

Materials and methods

Chemicals and antibodies

Unless otherwise specified, chemicals and reagents were purchased from Sigma Aldrich. Antibodies against: P21CIP1 (C-19) were purchased from Santa Cruz Biotechnology, KI-67 from Dako, PARP-1 from Enzo, E-CADHERIN, SNAIL, β-CATENIN and NANOG from Cell Signaling, GAPDH from Millipore, CYCLIN D1 from Thermo Scientific. Secondary anti-mouse and anti-rabbit antibodies conjugated with HRP were obtained from Vector Laboratories, and ECL reagents from Thermo Scientific. Secondary antibodies conjugated with AlexaFluor 488 or AlexaFluor 555 were purchased from Thermo Fisher Scientific. Mounting medium was obtained from Roche Diagnostics. 7-AAD, FITC mouse anti-human CD24, FITC mouse IgG2a, κ isotype control, AlexaFluor® 700 mouse IgG2b, κ isotype control, Alexa Fluor®700 mouse anti-human CD44 were obtained from BD Pharmingen™, APC mouse IgG1 isotype control, APC mouse anti-human CD133/1 (AC133) were purchased from Miltenyi Biotec. ELISA kits for human vascular endothelial growth factor (VEGF), and human interleukin-8 (IL-8) were procured from R&D Systems. Protein arrays were obtained from RayBiotech.

Cells and treatment

Human colon HCT116 cancer cells were kindly provided by Dr. Bert Vogelstein (Johns Hopkins University, Baltimore, MD). Authentication of cell lines was performed by Cell Line Authentication IdentiCell STR. Human colon cancer cell line SW480 was from ATCC. Cells were grown under standard conditions (37°C, 5% CO_2) in McCoy's medium supplemented with 10% fetal bovine serum, 10 000 units/mL of penicillin, 10 000 μg/mL of streptomycin, 100 ug/mL of streptomycin and 0.25 μg/mL of amphotericin B (Antibiotic-Antimycotic).

To induce senescence the cells were seeded at a density of 10 000/cm^2 24 hours before chemotherapeutics treatment. Next, colon cancer cells were cultured in the presence of 100 (HCT116) or 50 nM (SW480) doxorubicin (DOXO), 50 μM 5-fluorouracil (5-FU), 5 (HCT116) or 2.5 μM (SW480) oxaliplatin (OXA) or 2.5 (HCT116) or 5 μM (SW480) irinotecan (IRINO) for 24 hours followed by three days in fresh medium without a drug. This procedure was repeated six times (LONG CHEMO protocol). In parallel, after 3rd cycle cells were cultured in drug-free medium for two weeks. Medium was changed every four days (AFTER CHEMO protocol). Doses of OXA, 5-FU and IRINO used in experiments were chosen as most efficient to induce senescence, but not cell death, on base of: SA-β-gal staining, counting in Burker's chamber, BrdU incorporation assay, cell cycle analysis with PI staining, and LDH release assay (data not shown).

Western blotting

Cells were harvested into Laemmli SDS sample lysis buffer, sonicated and centrifuged at 10 000 x g. Concentration of proteins was estimated by the BCA method. 100 mM DTT and 0.01% bromophenol was added to lysates before separation by SDS-PAGE. The same protein amount was loaded into each well. Membranes were blocked in 5% non-fat milk and probed overnight at 4°C with antibodies specific for: P21CIP1 (1:500), PARP-1, SNAIL (1:500), CYCLIN D1, E-CADHERIN and β-CATENIN (1:1 000). GAPDH (1:30 000) or β-ACTIN (1:50 000) was used as a loading control. Then proteins were detected using appropriate secondary HRP-conjugated antibodies (1:10 000) and ECL reagents as recommended by manufacturer.

Detection of senescence-associated β-galactosidase (SA-β-Gal)

SA-β-Gal activity was detected according to modified Dimri et al.[32]. Briefly, cells were trypsinized, fixed with 2% formaldehyde, 0.2% glutaraldehyde in PBS, washed, cytospined and exposed overnight at 37°C to a solution containing 1 mg/ml 5-bromo-4-chloro-3-indolyl-b-D-galactopyranoside, 5 mM potassium ferrocyanide, 150 mM NaCl, 2 mM $MgCl_2$, and 0.1 M phosphate buffer, pH 6.0.

Enzyme-Linked Immunosorbent Assay (ELISA) for vascular endothelial growth factor (VEGF) and interleukin-8 (IL-8)

Concentrations of secreted proteins VEGF and IL-8 in the culture media were measured using a colorimetric ELISA according to the vendor's instructions. Tests were specific for human proteins. Results were normalized to total cell number.

Protein arrays

Concentrations of secreted proteins in the culture media were measured using a RayBiotech protein arrays (C-series) according to the vendor's instructions. Media were pooled from three to five independent experiments. We designed arrays for 60 cytokines related to: growth and differentiation, angiogenesis, inflammation, degradation of extracellular matrix, and adhesion. These were the following: EGF, Amphiregulin, Cripto-1, bFGF, TGF beta1, TGF beta2, TGF beta3, GDF-15, BMP-4,

HGF, IGF-I, IGF-II, IGFBP-3, Insulin, Leptin, LIF, NAP-2, S-100B, SCF, Shh-N, SDF-1 alpha, PDGF-AA, PDGF-AB, PDGF-BB, Angiogenin, Angiopoetin-1, Angiopoetin-2, Tie-1, Tie-2, Endoglin, Angiostatin, VE-cadherin, VEGF, VEGF-C, VEGF-D, CXCL10, G-CSF, M-CSF, GM-CSF, IL-10, IL-6, IL-8, MCP-1, GRO alpha, RANTES, ENA-78, Osteopontin, Resistin, MMP-2, MMP-9, TIMP-1, TIMP-2, Cathepsin S, uPA, PAI-I, EpCAM, ICAM-1, ICAM-2, ICAM-3, VCAM-1.

Images of the proteomic matrices were divided using a 10 × 14 square grid with the mesh corresponding to 1.15 of the diameter of the largest protein spot (positive control). The image intensities were integrated over the meshes and normalized (on the matrix-by-matrix basis) to the difference between the respective average integrals of the negative and positive controls. The normalized protein intensities, corresponding to the treated samples were divided by their counterparts of the non-treated samples and represented as a heatmap. The image processing and data visualization was implemented with Matlab R2016a.

Cell viability determination

Cell viability were assessed using Lactate dehydrogenase (LDH) release test according to the vendor's instructions. Results were normalized to the total cell number.

Matrigel assay

To test whether senescent cells can form tumorospheres, after 3rd chemotherapeutics cycle, alive, adherent HCT116 cells were replated into 96-well plates fulfilled with 50 μl of Matrigel Matrix (Growth Factor Reduced). Cells were seeded at a density of 1 000 cells per well and cultured for additional 21 days. Medium was changed every seven days. Untreated HCT116 cells were used as a control. Images of the spheres were taken using inverted Olympus DP73 microscope, working in transmitted light mode. All image processing operations were implemented using CellProfiler 2.1. as previously described.[25]

DNA content analysis

For DNA analysis cells were collected by trypsinization, fixed in 70% ethanol and stained with propidium iodide (PI) solution (3.8 mM sodium citrate, 50 mg/ml RNAse A, 500 mg/ml PI, in PBS). DNA content analyses were performed using a Becton-Dickinson FACS Calibur and the BD CellQuest Pro 6.0 software. At least 10 000 events were analyzed for each sample.

Side population (SP) evaluation

Cells were trypsinized, washed twice in PBS and then re-suspended at 10^6 cells/ml in PBS, then incubated at 37°C with 5 μg/ml Hoechst 33342 (H33342). Cells were incubated for 30 minutes at 37°C with constant mixing. Staining was halted by rinsing in ice-cold PBS. Prior to measurement cells were stained with PI (4 μM) for viability assessment. Data for 30 000 cells were analyzed using the BD LSRFortessa flow cytometer and BD FACSDiva 6.2 software as previously described.[25]

Flow cytometry analysis of cancer stem cell markers

Cells labeled with H33342 for SP were probed with specific fluorochrome-conjugated antibodies. Briefly, 1×10^5 cells were incubated with antibodies: APC-conjugated anti-CD133, FITC-conjugated anti-CD24 and AlexaFluor 700-conjugated anti-CD44 antibodies for 30 minutes on ice. Labeled cells were re-suspended in PBS and stained with PI (4 μM) for viability assessment. Isotypic IgGs served as a negative control. Flow cytometry was performed using a BD LSRForessa instrument and BD FACSDiva 6.2 software as previously described.[25]

Immunofluorescent staining

Cells grown on chamber slides were fixed with 4% formaldehyde, permeabilized with 0,5% Triton X-100 and blocked with 5% goat serum. Afterwards, cells were incubated with the primary antibodies at 1:100 in the blocking solution at 4°C overnight in humidified chamber. After that, samples were incubated with secondary antibodies conjugated with AlexaFluor 488 or AlexaFluor 555 diluted 1:200 in PBS. Then, the slides were stained with H33342 (1 μg/ml in PBS) and mounted with Fluorescent Mounting Medium. In the control experiments, the steps with primary antibodies were omitted. Images were captured using Leica DM4000B fluorescence microscope controlled by Image Pro-Plus 5.0 software.

Long-term time-lapse

Cells were seeded in 6-well plate and starting at indicated day of AFTER CHEMO protocol they were recorded for 48 hours. Transmitted light images (DIC – Nomarski contrast) were taken every 10 minutes using Leica AF7000 microscope equipped with 10x dry objective, DFC350 FX CCD camera (Leica, Mannheim, Germany), and environmental chamber (Pecon, Erbach, Germany).

Statistical analysis

In vitro experiments were performed in duplicates or triplicates and repeated at least three times. Numerical results are expressed with mean values ± standard errors. The respective p-values were calculated using type-2 two-tailed *t* (Student) test and $p < 0.05$ was considered statistically significant.

Results

Kinetics of cell re-population after chemotherapeutics withdrawal depends on the drug type

In our previous studies we found that human colon cancer HCT116 cells treated with doxorubicin (DOXO) undergo senescence in cell cultures, but after withdrawal of the drug re-growth is observed.[25,33,34] However, DOXO is not used in therapy of colon cancer patients. Thus, here we tested the effects of the clinically relevant chemotherapeutics: 5-fluorouracil (5-FU), oxaliplatin (OXA) and irinotecan (IRINO). We subjected HCT116 cells to six cycles of drug treatment in the long term cultures (Fig. 1A LONG CHEMO protocol), mimicking a regime of chemotherapy. Subsequently, to mimic a post-chemotherapy

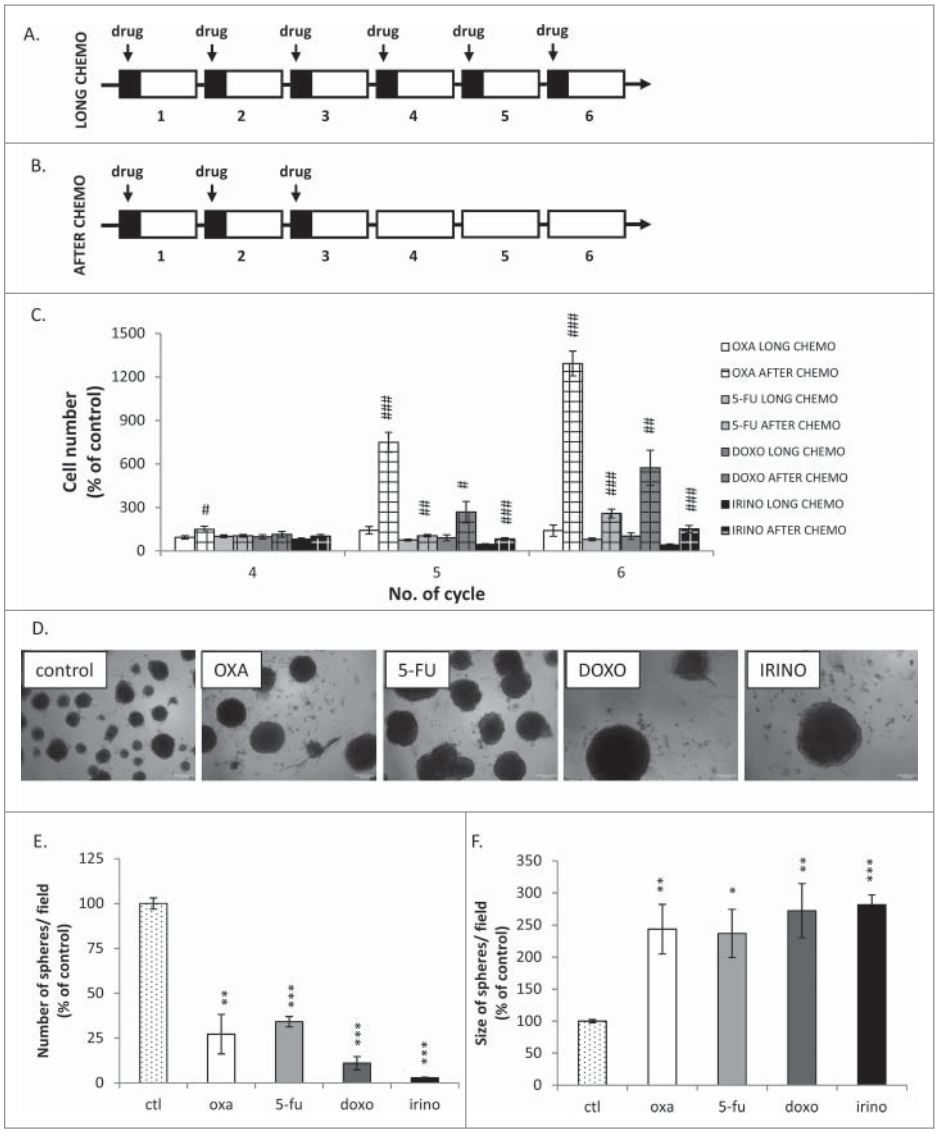

Figure 1. Kinetics of colon cancer cell re-population after chemotherapeutics withdrawal is a drug-specific. Experimental protocols. A. LONG CHEMO protocol. HCT116 cells were subjected to six cycles of chemotherapeutics as follows: cells were treated with 5 μM OXA, 100 nM DOXO, 50 μM 5-FU or 2.5 μM IRINO for 24 hours, then a medium was removed and cells were cultured in a drug-free medium for the next 3 days. B. AFTER CHEMO protocol. After 3rd drug treatment HCT116 cells were cultured in a drug-free medium for additional 14 days. C. Evaluation of cell number at various time points after drug treatment (AFTER CHEMO). DOXO at 100 nM concentration was used as a reference drug inducing senescence and after withdrawal – senescence escape.[25] D. Visualization of spheres formed by untreated and chemotherapeutics-treated cells. AFTER CHEMO-treated cells (1 000 cells/96-well plate) were harvested and seeded on the 14th day into matrigel. Representative photos were taken three weeks after seeding with light microscopy (100x magnification). E. Numbers of spheres formed by untreated or AFTER CHEMO-treated cells. F. Evaluation of size of spheres formed by untreated or AFTER CHEMO-treated cells. Each bar represents mean ± SEM, N≥3; statistical significance # – $p < 0,05$, ## – $p < 0,01$, ### – $p < 0,001$ – LONG CHEMO vs. AFTER CHEMO, *– $p < 0,05$, **– $p < 0,01$,>> ***– $p < 0,001$–untreated vs. AFTER CHEMO.

period, after 3rd drug cycle, we cultured HCT116 cells in drug-free medium for additional 14 days (Fig. 1B, AFTER CHEMO protocol). DOXO at 100 nM concentration was used as the reference drug for inducing senescence and, after withdrawal, senescence escape.[25,34]

We demonstrated different kinetics of cell re-population after drug removal, when the AFTER CHEMO protocol was applied (Fig. 1C). After OXA removal, the significant increase in the cell number was visible already at the 4th cycle. Then, at the 5th cycle the increase of the cell number was detectable also in cultures threated with other drugs. At the end of the 6th cycle the cell number after OXA removal was five times higher, when compared to DOXO, and ten times higher compared to 5-FU and IRINO, as shown in Fig. 1C. Additionally, we studied the effect of chemotherapeutic treatment on the spheroid-forming potential of individual HCT116 cells. For this purpose, we seeded cells at low density (1 000 cells per well) on the 14th day onto matrigel and examined their ability to form spheres three weeks later. In general, all four drugs produced the significant decrease in the number of spheres (Fig. 1D,E). On the other hand, the diameter of spheres formed by chemotherapeutics-treated (particularly DOXO and IRINO) cells was larger than in their untreated counterparts (Fig. 1D,F).

Using the LONG CHEMO protocol, we studied further the differences in response to chemotherapeutics by quantifying two processes, which affect cell number: cell death and proliferation. The LDH release test results indicated that all drugs have similar efficacy to induce cell death (Fig. 2A). Moreover, all drugs induced apoptosis at early stages of treatment, as demonstrated by the PARP-1 cleavage, measured with western blotting

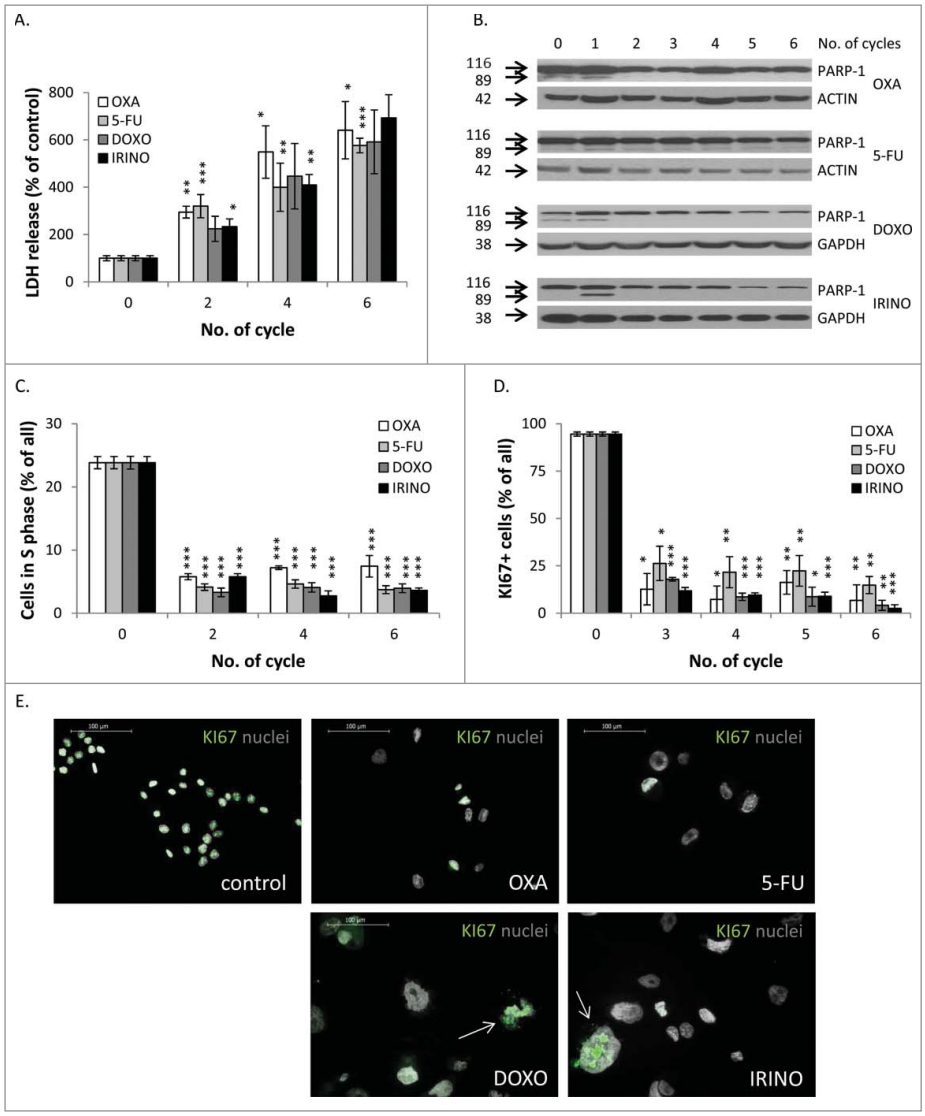

Figure 2. There are no differences in terms of cell death and proliferation after chemotherapeutics treatment. HCT116 cells were treated with LONG CHEMO protocol. A. Evaluation of cell mortality, performed using LDH assay. B. Representative blot shows expression of PARP-1. Cleaved form of PARP-1 (89 kDa) is the hallmark of apoptosis. GAPDH or ACTIN was used as a loading control. C. Fractions of cells in S phase, quantified with PI staining and flow cytometry. D. Fractions of KI67 positive cells. E. Representative photos show KI67 staining in untreated and OXA-, 5-FU-, DOXO- or IRINO-treated HCT116 cells: KI67 visualized as green (AlexaFluor 488), and nuclei visualized as grey (H33342). KI67^{+} polyploid cells indicated with white arrows. Data obtained with fluorescence microscopy (200x magnification) at the end of the 5th cycle of LONG CHEMO protocol. Scale bar – 100μm. Each bar represents mean ± SEM, N≥3; statistical significance * – $p < 0{,}05$, ** – $p < 0{,}01$, *** – $p < 0{,}001$ – untreated vs. LONG CHEMO.

(Fig. 2B). In addition, we showed that all drugs inhibited proliferation, as revealed by reduction in percentages of cells in the S phase of cell cycle (Fig. 2C). Correspondingly, treatment with drugs led to the significant decrease of the fraction of KI67 positive cells (Fig. 2D). The KI67 staining was detectable in some giant (presumably senescent) cells (Fig. 2E). Taken together, these data suggest that withdrawal of the chemotherapeutic drugs might lead to cancer cell re-growth, albeit kinetics of this process may differ between drugs. In particular, DOXO, 5-FU or IRINO might postpone onset of the process, finally increasing the proliferative potential of progeny within spheres.

Repeated cycles of DOXO, IRINO and partially 5-FU induce senescence of HCT116 cells

We did not find differences in the probability of death of HCT116 cells treated with different chemotherapeutics agents. Thus, we hypothesized that changes in the kinetics of cell repopulation might be related to induction of cellular senescence.[19] Indeed, we observed that the morphology of cells was affected differently by the studied drugs. Treatment with DOXO and IRINO resulted in the marked increase of the size of cells and their nuclei, whereas no such effects were produced by OXA. Cells treated with 5-FU exhibited the intermediate morphological changes (Fig. 3A). All drugs induced growth arrest (Fig. 2C, 2D and 3B) and the increase in cell granularity, as shown by SSC/FSC parameters measured by flow cytometry (Fig. 3C). It should be noted that treatment with DOXO and IRINO produced the largest HCT116 cells (Fig. 3A and 3D). Moreover, the SA-β-galactosidase activity was the most pronounced in these cells (Fig. 3D,E). The fraction of SA-β-gal positive cells increased with every cycle of 5-FU treatment (Fig. 3E). Next, we analyzed the cell cycle distribution using PI staining. Following DOXO or IRINO treatment, the

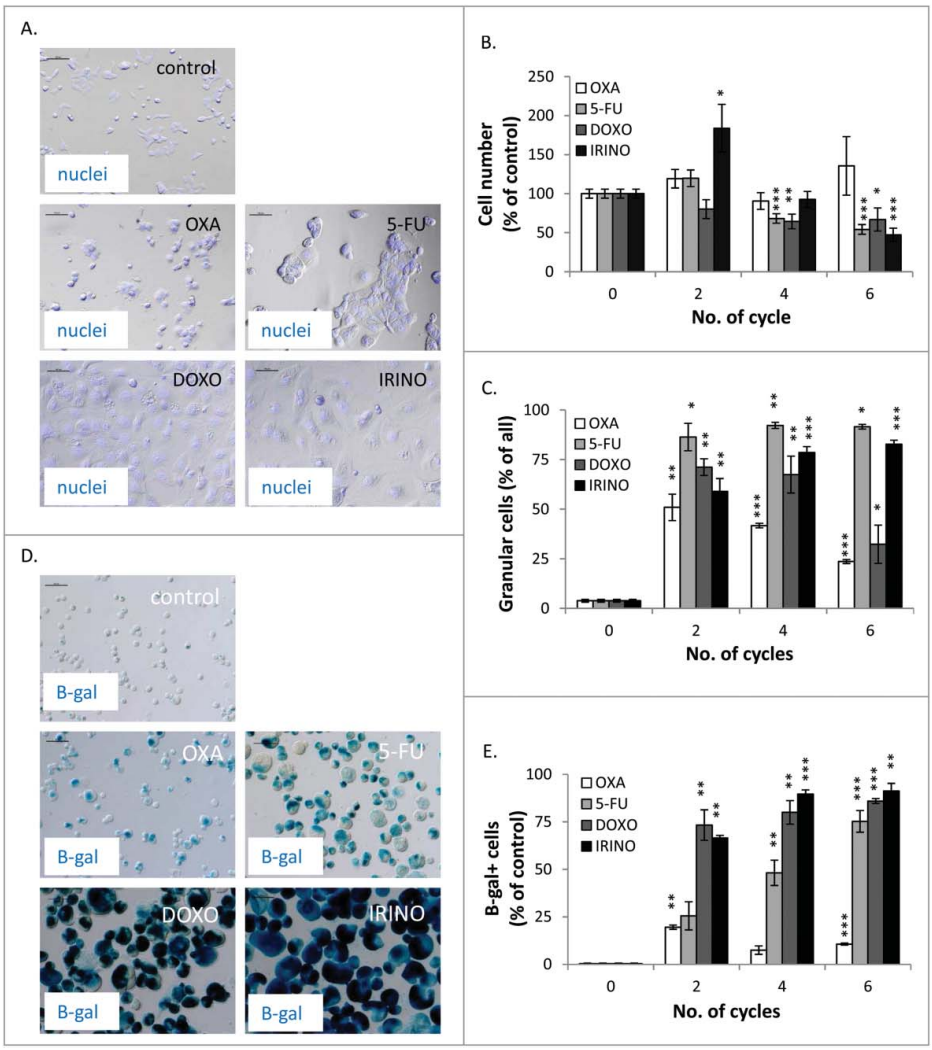

Figure 3. DOXO and IRINO are the strongest inducers of cellular senescence and activate its hallmarks: growth arrest, and an increase in size, granularity and SA-β-gal positivity. HCT116 cells were treated with LONG CHEMO protocol. A. Representative photos showing morphological alterations in OXA-, 5-FU-, DOXO- or IRINO-treated HCT116 cells. Cell nuclei were stained with H33342 dye (blue). Data acquired using fluorescence and transmitted light microscopy (200x magnification) at the end of the 5th cycle of LONG CHEMO protocol. Scale bar – 100μm. B. Evaluation of cell number at several time points after drug treatment. Cell were counted in Bürker's chamber. C. Fraction of granular cells as determined by FSC/SSC analysis, using flow cytometry. D. Representative photos of SA-β-gal staining on untreated and treated cells. Staining was performed on cytospined cells to enable easier quantification of SA-β-gal positive cells. Scale bar – 100μm. Data obtained with transmitted light microscopy (200x magnification) at the end of the 5th cycle of LONG CHEMO protocol. E. Fractions of SA-β-gal^{+} cells. Each bar represents mean ± SEM, N≥3; statistical significance * – $p < 0,05$, ** – $p < 0,01$, *** – $p < 0,001$ – untreated vs. LONG CHEMO.

percentages of diploid cells in G0/G1 phase of the cell cycle were significantly reduced (Fig. 4A). The DOXO treatment decreased also fractions of diploid cells in the G2/M phase and/or tetraploid cells arrested in the G0/G1 phase (Fig. 4B). Finally, DOXO or IRINO treatments produced the strongest increase in the fraction of polyploid cells (Fig. 4C). These data were corroborated with the measurements of expression of senescence-related proteins. We found that 5-FU, DOXO, or IRINO (Fig. 4D) treatment led to strong and prolonged accumulation of the cell cycle inhibitor – p21 and the geroconversion marker – CYCLIN D1.[35] One may note that senescent cells are also characterized by the senescence-associated secretory phenotype (SASP).[19] Correspondingly, we have previously demonstrated that HCT116 cells treated with DOXO produce IL-8 and VEGF, as a part of the SASP phenotype.[25,33] Here, we showed that repeated cycles of IRINO and especially DOXO led to the marked augmentation of VEGF (Fig. 4E) and IL-8 (Fig. 4F) secretion. To expand these studies, we designed protein arrays and examined secretion of 60 cytokines related to: growth, differentiation, angiogenesis, inflammation, degradation of extracellular matrix and adhesion. We found that treatment with all chemotherapeutics, especially those inducing senescence, down-regulated (in comparison to untreated controls) the production of the majority of these proteins (Fig. S1). Treatments with DOXO, IRINO or 5-FU led also to the increased secretion of cytostatic factors: amphiregulin and IGFBP-3 (Fig. S1A), as well as a proangiogenic factor: PDGF-AA (Fig. S1B). Moreover, HCT116 cells exposed to repeated cycles of those drugs produced more immunomodulatory cytokines: MCP-1, GRO-alpha and IL-10 (Fig. S1C), as well as proteases: uPA, PAI-I and inhibitors of metalloproteinases, especially TIMP-2 (Fig. S1D). Finally, cells treated with DOXO, IRINO or 5-FU secreted less adhesion molecules: ICAM-3 and V-CAM (Fig. S1E). To summarize, our data indicate that the repeated treatment with DOXO or IRINO induces senescence of HCT116 cells. Cells treated with 5-FU also developed the

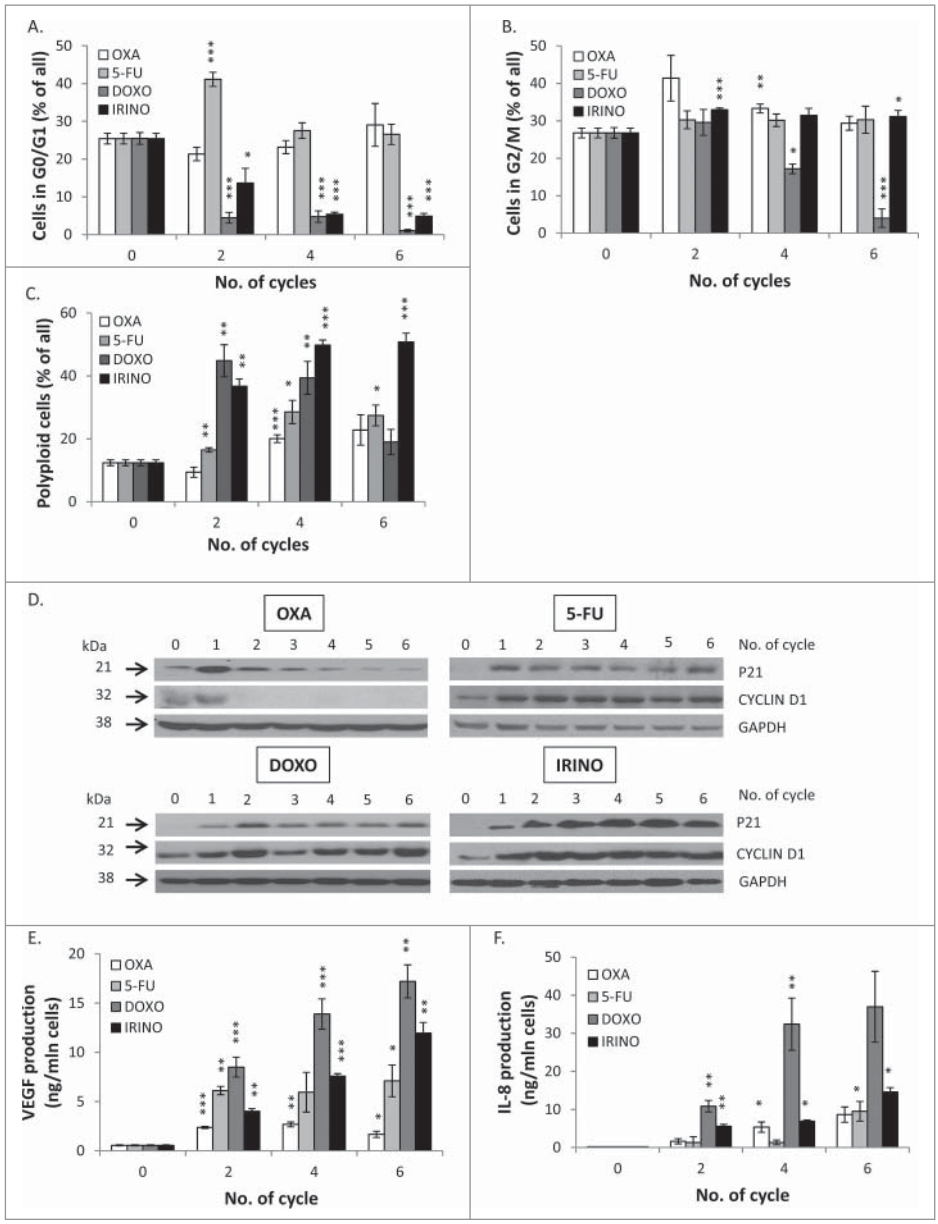

Figure 4. DOXO and IRINO are the strongest inducers of cellular senescence and activate its hallmarks: alternations of cell cycle, and an increase in expression levels of P21 and CYCLIN D1 as well as secretory phenotype. HCT116 cells were treated with LONG CHEMO protocol. Fractions of HCT116 cells in different phases of cell cycle after OXA, 5-FU, DOXO or IRINO treatment: A. G0/G1, B. G2/M and C. Fractions of polyploid cells. Cell cycle analysis was performed using PI staining and flow cytometry. D. Representative blots show expression levels of: P21 and CYCLIN D1 in OXA-, 5-FU-, DOXO- or IRINO-treated cells. GAPDH detection was used as a loading control. Secretion of E. VEGF and F. IL-8 in OXA-, 5-FU-, DOXO- or IRINO-treated HCT116 cultures. Cytokine levels were determined in supernatants harvested from untreated and treated cells by colorimetric ELISA. Results were normalized to total cell number counted in Bürker's chamber. Each bar represents mean ± SEM, N≥3; statistical significance * – $p < 0,05$, ** – $p < 0,01$, *** – $p < 0,001$ – untreated vs. LONG CHEMO.

senescent phenotype, albeit manifested after a larger number of treatment cycles.

Cancer cells treated with senescence-induced chemotherapeutics display several stemness features

Recently, it has been reported that senescent cancer cells may exhibit some features of stem cells.[21–23,25–27] This notion is compatible with the observed, elevated expression of a stem cell transcription factor NANOG in HCT116 cells subjected to repeated doses of 5-FU, DOXO or IRINO (Fig. 5A). It is worthy to note that NANOG was detected not only in cytoplasm, but also in nuclei of some giant cells (Fig. 5B), as demonstrated with immunofluorescence staining. The treatment with senescence-inducing agents increased also the number of cells identified as the side population, as determined by Hoechst 33342 exclusion assay (Fig. 6A). Moreover, the treatment with chemotherapeutics changed fractions of cells expressing cancer stem cell markers: CD24, CD44 and CD133. Treatments with DOXO or IRINO resulted in the marked increase of the CD24-positive cell fraction (Fig. 6B). The smaller increase was detected among the cells treated with 5-FU (Fig. 6B). The effect was the strongest among polyploid cells (Fig. S2A). Correspondingly, DOXO, IRINO or 5-FU reduced the fraction of the CD44-positive cells (Fig. 6C). The effect was the weakest among polyploid cells (Fig S2B). Furthermore, all tested drugs

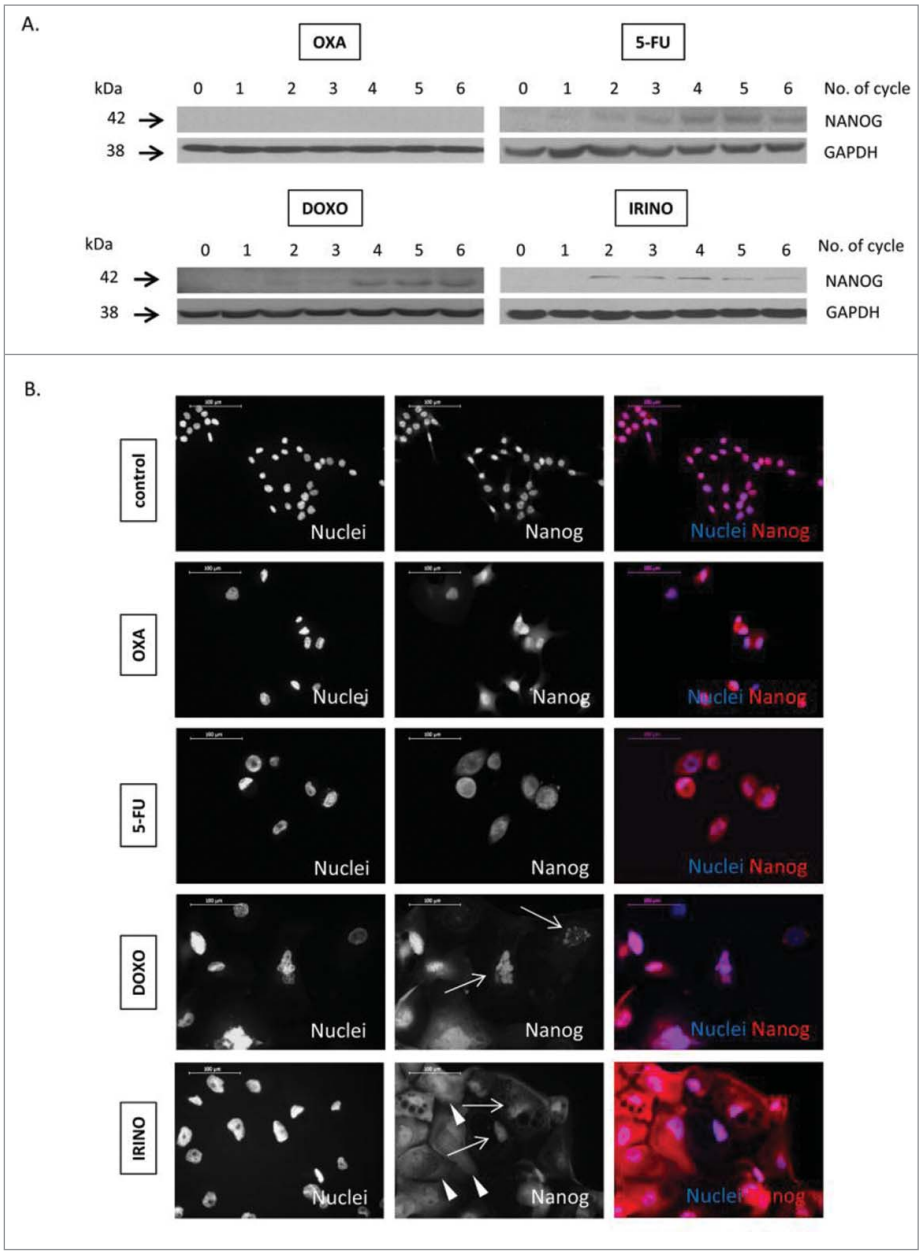

Figure 5. Some senescent HCT116 cells show elevated NANOG expression. HCT116 cells were treated with LONG CHEMO protocol. A. Representative blot shows the expression of NANOG in OXA-, 5-FU-, DOXO- or IRINO-treated HCT116 cultures. Membranes were re-probed with anti-GAPDH antibodies, which were used as loading controls. B. Representative photos show NANOG staining in untreated, OXA-, 5-FU-, DOXO- or IRINO-treated HCT116 cells: NANOG visualized as red (AlexaFluor 555), and nuclei visualized as blue (H33342). Nucelar NANOG localization in polyploid cells indicated with white arrows. Cytoplasmic NANOG localization in polyploid cells indicated with white arrowheads. Data obtained with fluorescent microscopy (200x magnification) at the end of 5th cycle of LONG CHEMO protocol. Scale bar – 100μm.

produced the decrease of the CD133-positive cell fraction (Fig. 6D).

To exclude that the observed changes were cell line-specific, we performed selected studies on another colon cancer cell line, SW480. As shown by the increased size and SA-β-gal staining, SW480 cells treated with DOXO or IRINO entered senescence (Fig. S3A). This process correlated with the increase of the side population characterized by Hoechst exclusion assay (Fig. S3B) and the fraction of the CD24-positive cells (Fig. S3C). Both, DOXO and IRINO produced the decrease of the CD44-positive fraction of SW480 cells (Fig. S3D).

Another feature of cancer stem cells is epithelial to mesenchymal transition (EMT), a process which facilitates metastasis.[36] Using western blotting analysis on a lysate of a whole cell population, we showed that the expression of the epithelial marker – E-CADHERIN was elevated after 5-FU, DOXO or IRINO (Fig. 6E). Correspondingly, the expression of SNAIL – an E-CADHERIN inhibitor and a mesenchymal marker, was strongly decreased upon 5-FU, DOXO or IRINO treatment (Fig. 6E). Both, E-CADHERIN (Fig. S4A) and β-CATENIN (Fig. S5A) were localized mostly in membrane and cytoplasm of giant cells. E-CADHERIN/β-CATENIN complex plays an important role in maintaining epithelial integrity.[37] Of note, not all senescent cells showed increased E-CADHERIN or β-CATENIN staining (Fig. S4A, S5A). Furthermore, the presence of ZEB-1, a mesenchymal marker, was detectable in nuclei of some polyploid cells (Fig. 7A). It is noteworthy that the rare giant cells exhibited blastocyst-like morphology,

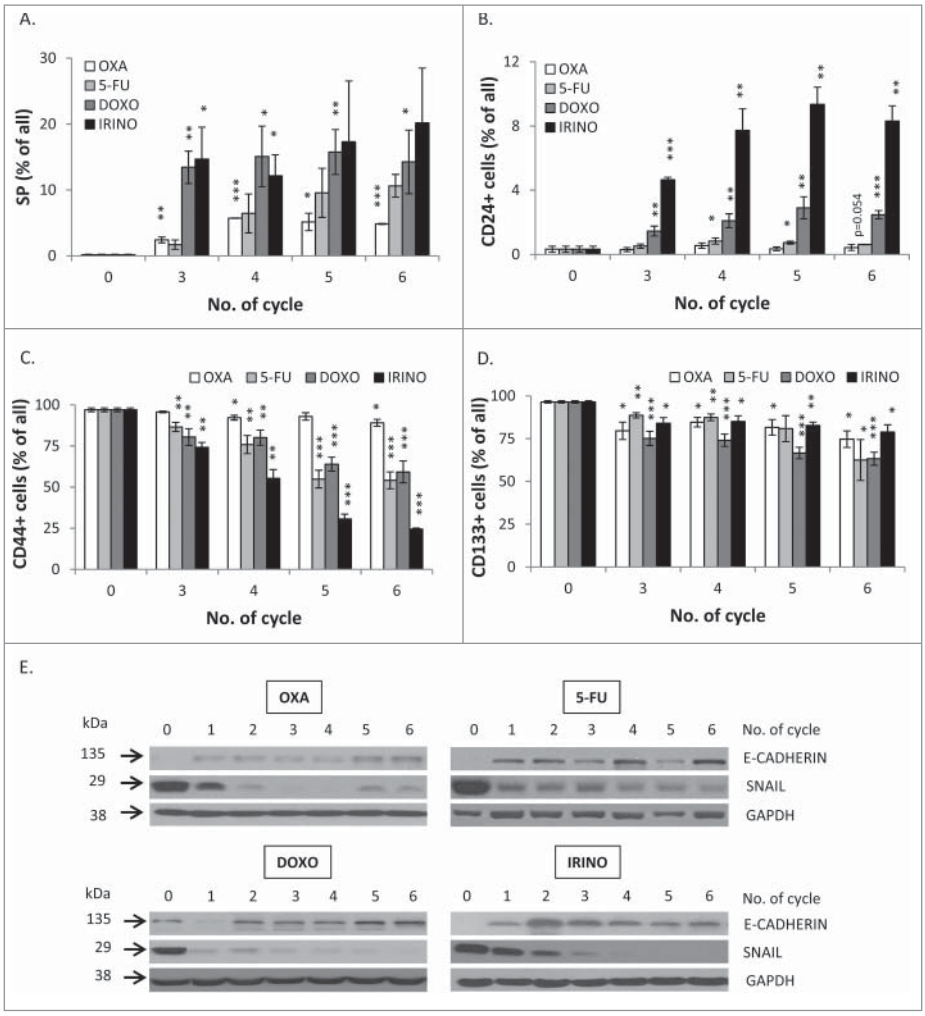

Figure 6. Senescent HCT116 cells show an increase in side population and fraction of CD24-positive, but reduced fraction of CD44-positive cells and decreased EMT. HCT116 cells were treated with LONG CHEMO protocol. A. Detection of cells excluding H33342. Cells treated with OXA-, 5-FU-, DOXO- or IRINO were stained with H33342 and analyzed by flow cytometry. Fractions of: B. CD24, C. CD44 or D. CD133 positive cells. Cells were probed with anti-CD24-FITC, anti-CD133-APC or anti-CD44-Alexa-Fluor700 antibodies and percentage of positive cells were determined using flow cytometry. Cells labeled with and isotypic IgGs were used as a negative control. E. The expression of epithelial to mesenchymal (EMT) markers in: OXA-, 5-FU-, DOXO- or IRINO-treated cells. Representative blots show expression levels of: E-CADHERIN and SNAIL. GAPDH detection was used as a loading control. Each bar represents mean ± SEM, N≥3; statistical significance * – $p < 0,05$, ** – $p<0,01$, *** – $p<0,001$ – untreated vs. LONG CHEMO.

reflected by big, round, floating body and the group of cells resembling an inner cell mass inside their cavities (Fig. 7C,D). ZEB-1 expression was also increased in some DOXO or IRINO-treated cells with a blastocyst-like morphology (Fig. 7B). Those structures appeared to be a source of progeny, characterized by a collective way of migration (Fig. 7D, Movie 1). To summarize, these data indicate that a subpopulation of senescent colon cancer cells display a specific phenotype being a mixture of stem-like and differentiated cell features.

Discussion

Cellular senescence has long been regarded as synergistic with cancer prevention and therapy.[38] However, recent data suggest that therapy-induced senescence (TIS) can lead to cancer recurrence in patients subjected to radio/chemotherapy.[15–17,19,39–41] Therefore, we studied induction of senescence by clinically used chemotherapeutics in human HCT116 and SW480 colon cancer cells *in vitro*. In the present study we showed that DOXO, IRINO or 5-FU treatment of colon cancer cells leads to accumulation of senescent cells exhibiting several features of stemness. These included the elevated NANOG levels, the significant increase in the side population and the augmented percentage of the CD24 positive cells. Surprisingly, the fraction of the CD44 positive cells was decreased, whereas levels of E-cadherin (epithelial marker) were increased. We observed some of these changes in another colon cancer cell line, SW480, which supports our conclusions and shows they are not restricted to a single cell line. Altogether, our results suggest that a subpopulation of senescent colon cancer cells display a specific phenotype comprising some stem-like and differentiated cell features. This notion is compatible with other studies, that demonstrated nuclear markers of stemness (OCT4, NANOG and SOX2) in rare, highly polyploid cells that may undergo meiosis-like depolyploidization and produce rejuvenated descendants.[22,42] Moreover, triploid breast cancer cells, non-responsive to neoadjuvant chemotherapy have been shown to contain the fraction of polyploid cells displaying both, NANOG and a cell cycle inhibitor p16 expression.[23] Furthermore, other data suggest that progeny emerging from polyploid cells may exhibit stem

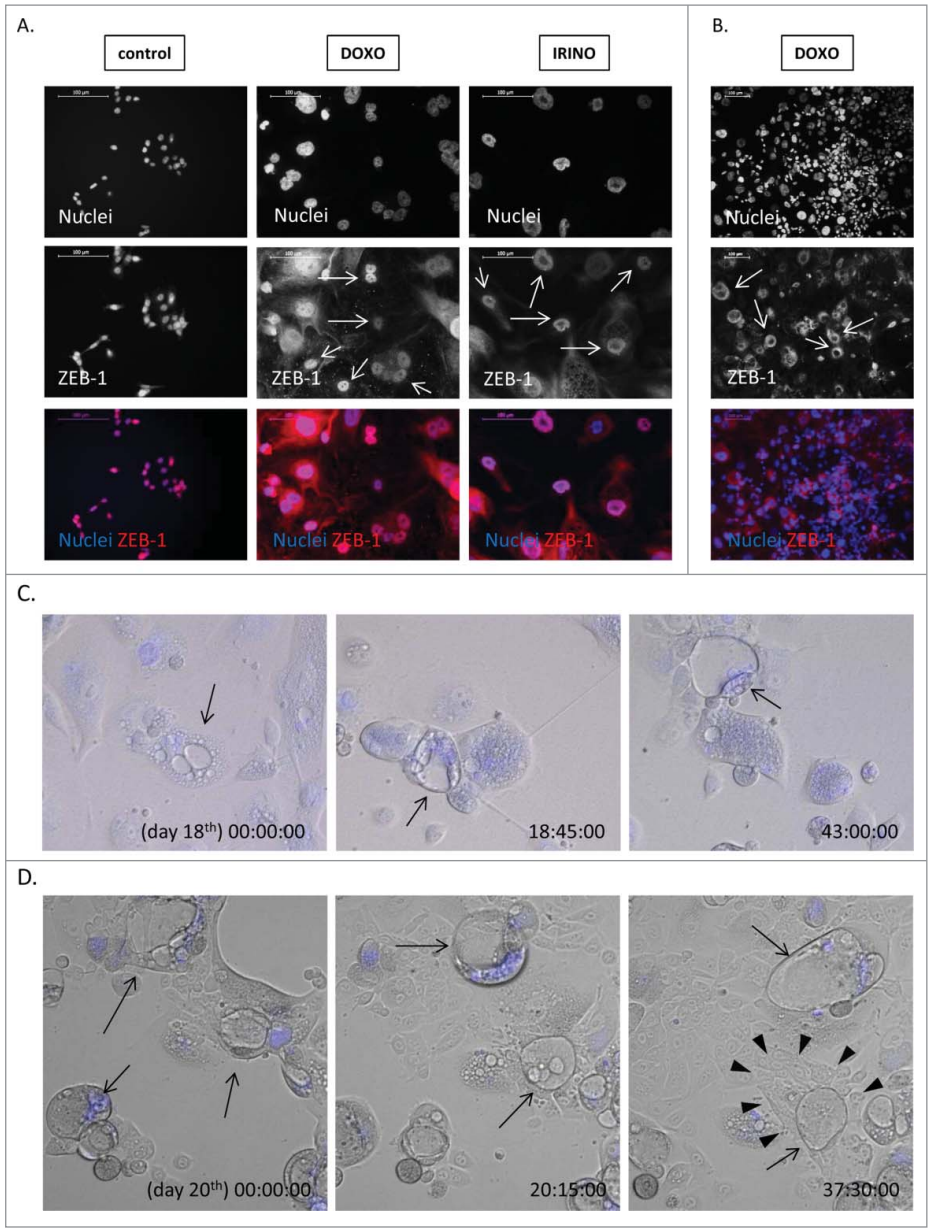

Figure 7. Some of polyploid HCT116 show ZEB-1 positivity and blastocyst-like morphology. HCT116 cells were treated with LONG CHEMO protocol. A. and B. Representative photos show ZEB-1 staining in untreated, DOXO- or IRINO-treated HCT116 cells: ZEB-1 visualized as red (AlexaFluor 555), and nuclei visualized as blue (H33342). ZEB-1 localization in nuclei of polyploid cells indicated by white arrows. Data obtained with fluorescent microscopy (200x magnification) at the end of 3rd or 5th cycle of LONG CHEMO protocol. Scale bar – 100μm. C. Polyploid cells show blastocyst-like morphology. These forms, indicated here by black arrows, consist of big, round, floating body and group of cells resembling inner cell mass inside their cavities. D. Polyploid cells with blastocyst-like morphology seem to be a source of progeny, that exhibit collective way of migration. Polyploid cells with blastocyst-like morphology are indicated by black arrows, whereas progeny migrating in collective way are indicated by white arrowheads. Cells were seeded in 6-well plate and treated with the AFTER CHEMO protocol. Cells had being recorded starting from the indicated day. Pictures were taken every 10 minutes for the next 48 hours using time-lapse microscopy in DIC Nomarski contrast mode, at 200x magnification. Nuclei visualized as blue (H33342).

cell-like characteristics and extended life span.[20,24,43] One may also note that polyploid giant cancer cells (PGCC) are positive for normal and cancer stem cell markers and exhibit asymmetric cell division. Single PGCC may produce spheroids *in vitro* and generate tumors in immunodeficient mice.[27] These data support our findings that treatment with chemotherapeutics leads to the increased amount of polyploid cells with stem cell-like properties within colon cancer cells.

We demonstrated that induction of senescence in colon cancer cells, detected with multiple markers, correlates with the increase of the fraction of the CD24 positive cells, but the decreased fraction of the CD44 positive cells. CD24 is involved in cell differentiation, but its expression and distribution in colorectal cancer is a subject of dispute. Nonetheless, previous studies have shown that 50–68% of patients with colorectal cancers expressed high CD24 levels.[44] Furthermore, CD24 positive subpopulations from colon cancer cell-lines exhibit stem cell-like properties.[45] In turn, CD44 is postulated to mediate a critical step in colon cancer metastasis.[46] Du et al.[47] indicated CD44 as a potential marker for CSCs in colorectal cancer, and HCT116 cells with the high expression of CD44 and CD133 have been shown to display tumor-initiating capability.[48] Recently, the presence of polyploid cells, characterized by CD44 positivity, mesenchymal-like phenotype, SOX2, OCT4, and NANOG expression has been correlated with the lack of response to chemotherapy and the poor survival prognosis of

breast cancer patients.[23] Our data indicate that senescence-inducing drugs, especially DOXO and IRINO, significantly increased the fraction of CD24 positive cells mostly among polyploid cells. In parallel, the reduction of the CD44 positive fraction was higher in diploid than in polyploid cells. As we shown previously, after DOXO removal the fraction of the CD44 positive diploid cells returned to the high basal level. Conversely, further reduction was observed in polyploid cells.[25] These data suggest that chemotherapeutics-treated colon cancer cells exhibit dynamic changes in CD24 and CD44 expression that may depend on cell ploidy. We postulate that it should be taken under consideration, when designing the CSC-targeted immunotherapy. Altogether, our data are in line with conclusions based on recent discoveries within the CSC field, that include: variability of CSC phenotypes, and potential of non-CSCs to switch to CSC-like cells in response to microenvironment signals.[28]

Importantly, here we show that some senescent colon cancer cells display the increased expression of mesenchymal marker, ZEB-1 (Zinc finger E-box binding homeobox 1) protein. EMT has been demonstrated to be a necessary step in tumor invasion and metastasis[49], whereas ZEB-1 can promote migration and invasion by inducing EMT.[50,51] CSCs may undergo EMT, thereby acquiring mesenchymal features, migrating to adjacent stromal tissues, and invading blood or lymph vessels. On the other hand, recent studies showed that EMT-inducible factors also trigger CSC-like features in cancer cells.[52] Additionally, ZEB-1 has been reported to enhance tumor radioresistance, in EMT independent pathway, which relies on the ATM−ZEB1−CHK1 signaling axis.[53–55] It is compatible with our observations that senescent HCT116 cells show the higher side population (SP) fraction than their untreated counterparts. The SP cells isolated from CRC cell line were shown to exhibit increased level of multidrug resistance.[56,57] It is likely that these cells were in the G0 phase (KI67 negative). It may be postulated that such quiescent or slow cycling CSCs may survive therapeutic intervention and produce a relapse.[28] Intriguingly, here we observed that rare, polyploid colon cancer cells might show the blastocyst-like morphology. In accordance, PGCCs derived from ovarian cancer cells and blastomeres were demonstrated to be equivalent.[58] The embryonic origin of cancer was conceptualized by Cohnheim in 1867, and then confirmed experimentally by Stevens[59,60] and Pierce.[61,62] Blastomeres, which are produced by cleavage of the zygote in the human preimplantation embryo, frequently exhibit a combination of diploidy and polyploidy.[63,64] Polyploid giant cells were postulated to have a distinct advantage over diploid cancer cells in coping with stresses and reproduction.[65] For instance, polyploidy has recently reported to induce docetaxel[66] and paclitaxel[58] resistance and escape from doxorubicin-induced senescence.[33] Altogether, our data suggest that senescence of cancer cells could be considered as a mechanism responsible for cancer relapse after chemotherapy.

Moreover, we demonstrate that majority of DOXO- and IRINO-treated colon cancer cells show the increased E-CADHERIN and reduced SNAIL expression, suggesting that these cells underwent mesenchymal to epithelial transition (MET). In accordance, they produce fewer spheres in matrigel than the untreated cells, indicating more dormant phenotype. This observation is supported by our previous *in vivo* data, showing that DOXO treatment resulted in delayed growth of tumors in NOD/SCID mice.[25] Strong correlation between senescence and MET was demonstrated in many experimental settings.[36] In line with our studies, oncogene-induced senescence and p21WAF1 escape observed in human colon adenocarcinoma[67] and in breast cancer cell lines[68] was associated with an induction of the EMT and an increase in the proportion of cells with the CD24low/CD44high phenotype. Moreover, paclitaxel-treated MCF-7 cells exhibited slow proliferation, low rates of invasion and reduced tumor formation.[26] Interestingly, we demonstrated that induction of autophagy may trigger proliferative potential of DOXO-treated colon cancer cells, both *in vitro* and in NOD/SCID mice.[25] One may speculate that accumulation of E-CADHERIN and β-CATENIN at the plasma membrane after DOXO and IRINO treatment forms an additional mechanical barrier in senescent cells. β-CATENIN is recruited by E-CADHERIN, and forms a protein complex involved in adherens junctions, which strengthens cell-cell and cell-surface contacts.[37] Therefore, a subpopulation of senescent cancer cells may play a supportive and protective role within a tumor. In this capacity they might be similar to the spores of lower organisms.[69,70]

We conclude that certain clinically used drugs induce senescence in colon cancer cells. Some senescent cells may display a specific phenotype being a combination of stem-like and differentiated cell features, which makes them tumor-initiating cells. Therefore, we propose that senescence of cancer cells should be carefully considered as a therapy-resistant mechanism, however the link between senescence and stemness requires further investigation.

Conflict of interest

The authors declare that they have no conflict of interest.

Grant support

This work was supported by the Foundation for Polish Science co-financed by the European Union under the European Social Fund – grant 125/UD/SKILLS/2013 (H.W.), the Ministry of Science and Higher Education – grant IP2012 062172 (H.W.) and NCN (Polish National Center of Science) – grants 2013/09/B/NZ3/01389 (T.B.) and 2012/05/E/ST2/02180 (T.B.). H. W. is the recipient of a fellowship from EU FP7 Project BIO-IMAGINE: BIO-IMAGing in research INnovation and Education, GA No. 264173 that was obtained by Nencki Institute of Experimental Biology. H.W. is the recipient of a scholarship for young and outstanding investigators from the Ministry of Science and Higher Education-scholarship no. 438/2012.

Acknowledgments

Flow cytometry analyses were performed at the Laboratory of Cytometry at the Nencki Institute.

Funding

The Foundation for Polish Science co-financed by the European Union under the European Social Fund (IP2012 062172); the Ministry of Science and Higher Education (IP2012 062172); the Ministry of Science and Higher Education (438/2012); Polish National Center of Science (2012/05/E/ST2/02180); Polish National Center of Science (2013/09/B/NZ3/01389); EU FP7 Project BIO-IMAGINE: BIO-IMAGing in research INnovation and Education (264173).

References

1. Jemal A, Siegel R, Ward E, Hao Y, Xu J, Murray T, Thun MJ. Cancer statistics, 2008. CA Cancer J Clin. 2008;58:71–96. doi:10.3322/CA.2007.0010.
2. Segal NH, Saltz LB. Evolving treatment of advanced colon cancer. Annu Rev Med. 2009;60:207–19. doi:10.1146/annurev.med.60.041807.132435.
3. Grothey A, Sargent D, Goldberg RM, Schmoll HJ. Survival of patients with advanced colorectal cancer improves with the availability of fluorouracil-leucovorin, irinotecan, and oxaliplatin in the course of treatment. J Clin Oncol. 2004;22:1209–14. doi:10.1200/JCO.2004.11.037.
4. Tournigand C, Andre T, Achille E, Lledo G, Flesh M, Mery-Mignard D, Quinaux E, Couteau C, Buyse M, Ganem G, et al. FOLFIRI followed by FOLFOX6 or the reverse sequence in advanced colorectal cancer: a randomized GERCOR study. J Clin Oncol. 2004;22:229–37. doi:10.1200/JCO.2004.05.113.
5. Boyer J, McLean EG, Aroori S, Wilson P, McCulla A, Carey PD, Longley DB, Johnston PG. Characterization of p53 wild-type and null isogenic colorectal cancer cell lines resistant to 5-fluorouracil, oxaliplatin, and irinotecan. Clin Cancer Res. 2004;10:2158–67. doi:10.1158/1078-0432.CCR-03-0362.
6. Curtin NJ, Harris AL, Aherne GW. Mechanism of cell death following thymidylate synthase inhibition: 2′-deoxyuridine-5′-triphosphate accumulation, DNA damage, and growth inhibition following exposure to CB3717 and dipyridamole. Cancer Res. 1991;51:2346–52.
7. Peters GJ, van Triest B, Backus HH, Kuiper CM, van der Wilt CL, Pinedo HM. Molecular downstream events and induction of thymidylate synthase in mutant and wild-type p53 colon cancer cell lines after treatment with 5-fluorouracil and the thymidylate synthase inhibitor raltitrexed. Eur J Cancer. 2000;36:916–24. doi:10.1016/S0959-8049(00)00026-5.
8. Kelland L. The resurgence of platinum-based cancer chemotherapy. Nat Rev Cancer. 2007;7:573–84. doi:10.1038/nrc2167.
9. Pommier Y. Topoisomerase I inhibitors: camptothecins and beyond. Nat Rev Cancer. 2006;6:789–802. doi:10.1038/nrc1977.
10. Kastan MB, Lim DS. The many substrates and functions of ATM. Nat Rev Mol Cell Biol. 2000;1:179–86. doi:10.1038/35043058.
11. Bakkenist CJ, Kastan MB. DNA damage activates ATM through intermolecular autophosphorylation and dimer dissociation. Nature. 2003;421:499–506. doi:10.1038/nature01368.
12. Giacchetti S, Perpoint B, Zidani R, Le Bail N, Faggiuolo R, Focan C, Chollet P, Llory JF, Letourneau Y, Coudert B, et al. Phase III multicenter randomized trial of oxaliplatin added to chronomodulated fluorouracil-leucovorin as first-line treatment of metastatic colorectal cancer. J Clin Oncol. 2000;18:136–47. doi:10.1200/JCO.2000.18.1.136.
13. Douillard JY, Cunningham D, Roth AD, Navarro M, James RD, Karasek P, Jandik P, Iveson T, Carmichael J, Alakl M, et al. Irinotecan combined with fluorouracil compared with fluorouracil alone as first-line treatment for metastatic colorectal cancer: a multicentre randomised trial. Lancet. 2000;355:1041–7. doi:10.1016/S0140-6736(00)02034-1.
14. Dahan L, Sadok A, Formento JL, Seitz JF, Kovacic H. Modulation of cellular redox state underlies antagonism between oxaliplatin and cetuximab in human colorectal cancer cell lines. Br J Pharmacol. 2009;158:610–20. doi:10.1111/j.1476-5381.2009.00341.x.
15. Wu PC, Wang Q, Grobman L, Chu E, Wu DY. Accelerated cellular senescence in solid tumor therapy. Exp Oncol. 2012;34:298–305.
16. Roberson RS, Kussick SJ, Vallieres E, Chen SY, Wu DY. Escape from therapy-induced accelerated cellular senescence in p53-null lung cancer cells and in human lung cancers. Cancer Res. 2005;65:2795–803. doi:10.1158/0008-5472.CAN-04-1270.
17. Wu PC, Wang Q, Dong ZM, Chu E, Roberson RS, Ivanova IC, Wu DY. Expression of coxsackie and adenovirus receptor distinguishes transitional cancer states in therapy-induced cellular senescence. Cell Death Dis. 2010;1:e70. doi:10.1038/cddis.2010.47.
18. Kuilman T, Michaloglou C, Mooi WJ, Peeper DS. The essence of senescence. Genes Dev. 2010;24:2463–79. doi:10.1101/gad.1971610.
19. Campisi J, d'Adda di Fagagna F. Cellular senescence: when bad things happen to good cells. Nat Rev Mol Cell Biol. 2007;8:729–40. doi:10.1038/nrm2233.
20. Sundaram M, Guernsey DL, Rajaraman MM, Rajaraman R. Neosis: a novel type of cell division in cancer. Cancer Biol Ther. 2004;3:207–18. doi:10.4161/cbt.3.2.663.
21. Erenpreisa J, Cragg MS. Three steps to the immortality of cancer cells: senescence, polyploidy and self-renewal. Cancer Cell Int. 2013;13:92. doi:10.1186/1475-2867-13-92.
22. Erenpreisa J, Salmina K, Huna A, Kosmacek EA, Cragg MS, Ianzini F, Anisimov AP. Polyploid tumour cells elicit paradiploid progeny through depolyploidizing divisions and regulated autophagic degradation. Cell Biol Int. 2011;35:687–95. doi:10.1042/CBI20100762.
23. Gerashchenko BI, Salmina K, Eglitis J, Huna A, Grjunberga V, Erenpreisa J. Disentangling the aneuploidy and senescence paradoxes: a study of triploid breast cancers non-responsive to neoadjuvant therapy. Histochem Cell Biol. 2016;145:497–508.
24. Rajaraman R, Guernsey DL, Rajaraman MM, Rajaraman SR. Stem cells, senescence, neosis and self-renewal in cancer. Cancer Cell Int. 2006;6:25. doi:10.1186/1475-2867-6-25.
25. Was H, Barszcz K, Czarnecka J, Kowalczyk A, Bernas T, Uzarowska E, Koza P, Klejman A, Piwocka K, Kaminska B, et al. Bafilomycin A1 triggers proliferative potential of senescent cancer cells in vitro and in NOD/SCID mice. Oncotarget. 2017;8:9303–22.
26. Zhang S, Mercado-Uribe I, Liu J. Tumor stroma and differentiated cancer cells can be originated directly from polyploid giant cancer cells induced by paclitaxel. Int J Cancer. 2014;134:508–18. doi:10.1002/ijc.28319.
27. Zhang S, Mercado-Uribe I, Xing Z, Sun B, Kuang J, Liu J. Generation of cancer stem-like cells through the formation of polyploid giant cancer cells. Oncogene. 2014;33:116–28. doi:10.1038/onc.2013.96.
28. Visvader JE, Lindeman GJ. Cancer stem cells: current status and evolving complexities. Cell Stem Cell. 2012;10:717–28. doi:10.1016/j.stem.2012.05.007.
29. Ricci-Vitiani L, Lombardi DG, Pilozzi E, Biffoni M, Todaro M, Peschle C, De Maria R. Identification and expansion of human colon-cancer-initiating cells. Nature. 2007;445:111–5. doi:10.1038/nature05384.
30. O'Brien CA, Pollett A, Gallinger S, Dick JE. A human colon cancer cell capable of initiating tumour growth in immunodeficient mice. Nature. 2007;445:106–10.
31. Dalerba P, Dylla SJ, Park IK, Liu R, Wang X, Cho RW, Hoey T, Gurney A, Huang EH, Simeone DM, et al. Phenotypic characterization of human colorectal cancer stem cells. Proc Natl Acad Sci U S A. 2007;104:10158–63. doi:10.1073/pnas.0703478104.
32. Dimri GP, Lee X, Basile G, Acosta M, Scott G, Roskelley C, Medrano EE, Linskens M, Rubelj I, Pereira-Smith O, et al. A biomarker that identifies senescent human cells in culture and in aging skin in vivo. Proc Natl Acad Sci U S A. 1995;92:9363–7. doi:10.1073/pnas.92.20.9363.
33. Mosieniak G, Sliwinska MA, Alster O, Strzeszewska A, Sunderland P, Piechota M, Was H, Sikora E, et al. Polyploidy Formation in Doxorubicin-Treated Cancer Cells Can Favor Escape from Senescence. Neoplasia. 2015;17:882–93. doi:10.1016/j.neo.2015.11.008.
34. Sliwinska MA, Mosieniak G, Wolanin K, Babik A, Piwocka K, Magalska A, Szczepanowska J, Fronk J, Sikora E. Induction of senescence with doxorubicin leads to increased genomic instability of HCT116 cells. Mech Ageing Dev. 2009;130:24–32. doi:10.1016/j.mad.2008.04.011.
35. Blagosklonny MV. Cell cycle arrest is not yet senescence, which is not just cell cycle arrest: terminology for TOR-driven aging. Aging (Albany NY). 2012;4:159–65.
36. Smit MA, Peeper DS. Epithelial-mesenchymal transition and senescence: two cancer-related processes are crossing paths. Aging (Albany NY). 2010;2:735–41.
37. Brembeck FH, Rosario M, Birchmeier W. Balancing cell adhesion and Wnt signaling, the key role of beta-catenin. Curr Opin Genet Dev. 2006;16:51–9. doi:10.1016/j.gde.2005.12.007.
38. Kong Y, Cui H, Ramkumar C, Zhang H. Regulation of senescence in cancer and aging. J Aging Res. 2011;2011:963172. doi:10.4061/2011/963172.
39. Gibadulinova A, Pastorek M, Filipcik P, Radvak P, Csaderova L, Vojtesek B, Pastorekova S. Cancer-associated S100P protein binds and inactivates p53, permits therapy-induced senescence and supports chemoresistance. Oncotarget. 2016;7:22508–22. doi:10.18632/oncotarget.7999.

40. Tato-Costa J, Casimiro S, Pacheco T, Pires R, Fernandes A, Alho I, Pereira P, Costa P, Castelo HB, Ferreira J, et al. Therapy-Induced Cellular Senescence Induces Epithelial-to-Mesenchymal Transition and Increases Invasiveness in Rectal Cancer. Clin Colorectal Cancer. 2016;15:170–8 e3. doi:10.1016/j.clcc.2015.09.003.
41. Ewald JA, Desotelle JA, Wilding G, Jarrard DF. Therapy-induced senescence in cancer. J Natl Cancer Inst. 2010;102:1536–46. doi:10.1093/jnci/djq364.
42. Salmina K, Jankevics E, Huna A, Perminov D, Radovica I, Klymenko T, Ivanov A, Jascenko E, Scherthan H, Cragg M, et al. Up-regulation of the embryonic self-renewal network through reversible polyploidy in irradiated p53-mutant tumour cells. Exp Cell Res. 2010;316:2099–112. doi:10.1016/j.yexcr.2010.04.030.
43. Rajaraman R, Rajaraman MM, Rajaraman SR, Guernsey DL. Neosis–a paradigm of self-renewal in cancer. Cell Biol Int. 2005;29:1084–97. doi:10.1016/j.cellbi.2005.10.003.
44. Weichert W, Denkert C, Burkhardt M, Gansukh T, Bellach J, Altevogt P, Dietel M, Kristiansen G. Cytoplasmic CD24 expression in colorectal cancer independently correlates with shortened patient survival. Clin Cancer Res. 2005;11:6574–81. doi:10.1158/1078-0432.CCR-05-0606.
45. Ke J, Wu X, Wu X, He X, Lian L, Zou Y, He X, Wang H, Luo Y, Wang L, et al. A subpopulation of CD24(+) cells in colon cancer cell lines possess stem cell characteristics. Neoplasma. 2012;59:282–8. doi:10.4149/neo_2012_036.
46. Marhaba R, Zoller M. CD44 in cancer progression: adhesion, migration and growth regulation. J Mol Histol. 2004;35:211–31.
47. Du L, Wang H, He L, Zhang J, Ni B, Wang X, Jin H, Cahuzac N, Mehrpour M, Lu Y, et al. CD44 is of functional importance for colorectal cancer stem cells. Clin Cancer Res. 2008;14:6751–60. doi:10.1158/1078-0432.CCR-08-1034.
48. Chen KL, Pan F, Jiang H, Chen JF, Pei L, Xie FW, Liang HJ. Highly enriched CD133(+)CD44(+) stem-like cells with CD133(+)CD44(high) metastatic subset in HCT116 colon cancer cells. Clin Exp Metastasis. 2011;28:751–63. doi:10.1007/s10585-011-9407-7.
49. Thiery JP, Sleeman JP. Complex networks orchestrate epithelial-mesenchymal transitions. Nat Rev Mol Cell Biol. 2006;7:131–42. doi:10.1038/nrm1835.
50. Peinado H, Olmeda D, Cano A. Snail, Zeb and bHLH factors in tumour progression: an alliance against the epithelial phenotype? Nat Rev Cancer. 2007;7:415–28. doi:10.1038/nrc2131.
51. Witta SE, Gemmill RM, Hirsch FR, Coldren CD, Hedman K, Ravdel L, Helfrich B, Dziadziuszko R, Chan DC, Sugita M, et al. Restoring E-cadherin expression increases sensitivity to epidermal growth factor receptor inhibitors in lung cancer cell lines. Cancer Res. 2006;66:944–50. doi:10.1158/0008-5472.CAN-05-1988.
52. Ishiwata T. Cancer stem cells and epithelial-mesenchymal transition: Novel therapeutic targets for cancer. Pathol Int. 2016;66:601–8. doi:10.1111/pin.12447.
53. Zhang P, Wei Y, Wang L, Debeb BG, Yuan Y, Zhang J, Yuan J, Wang M, Chen D, Sun Y, et al. ATM-mediated stabilization of ZEB1 promotes DNA damage response and radioresistance through CHK1. Nat Cell Biol. 2014;16:864–75. doi:10.1038/ncb3013.
54. Zhang P, Sun Y, Ma L. ZEB1: at the crossroads of epithelial-mesenchymal transition, metastasis and therapy resistance. Cell Cycle. 2015;14:481–7. doi:10.1080/15384101.2015.1006048.
55. Cortez MA, Valdecanas D, Zhang X, Zhan Y, Bhardwaj V, Calin GA, Komaki R, Giri DK, Quini CC, Wolfe T, et al. Therapeutic delivery of miR-200c enhances radiosensitivity in lung cancer. Mol Ther. 2014;22:1494–503. doi:10.1038/mt.2014.79.
56. Xiong B, Ma L, Hu X, Zhang C, Cheng Y. Characterization of side population cells isolated from the colon cancer cell line SW480. Int J Oncol. 2014;45:1175–83. doi:10.3892/ijo.2014.2498.
57. Haraguchi N, Utsunomiya T, Inoue H, Tanaka F, Mimori K, Barnard GF, Mori M. Characterization of a side population of cancer cells from human gastrointestinal system. Stem Cells. 2006;24:506–13. doi:10.1634/stemcells.2005-0282.
58. Niu N, Mercado-Uribe I, Li J. Dedifferentiation into blastomere-like cancer stem cells via formation of polyploid giant cancer cells. Oncogene. 2017;. doi:10.1038/onc.2017.72.
59. Stevens LC, Little CC. Spontaneous Testicular Teratomas in an Inbred Strain of Mice. Proc Natl Acad Sci U S A. 1954;40:1080–7. doi:10.1073/pnas.40.11.1080.
60. Stevens LC. Experimental Production of Testicular Teratomas in Mice. Proc Natl Acad Sci U S A. 1964;52:654–61. doi:10.1073/pnas.52.3.654.
61. Kleinsmith LJ, Pierce GB, Jr. Multipotentiality of Single Embryonal Carcinoma Cells. Cancer Res. 1964;24:1544–51.
62. Pierce GB, Speers WC. Tumors as caricatures of the process of tissue renewal: prospects for therapy by directing differentiation. Cancer Res. 1988;48:1996–2004.
63. Chavez SL, Loewke KE, Han J, Moussavi F, Colls P, Munne S, Behr B, Reijo Pera RA. Dynamic blastomere behaviour reflects human embryo ploidy by the four-cell stage. Nat Commun. 2012;3:1251. doi:10.1038/ncomms2249.
64. Kligman I, Benadiva C, Alikani M, Munne S. The presence of multinucleated blastomeres in human embryos is correlated with chromosomal abnormalities. Hum Reprod. 1996;11:1492–8. doi:10.1093/oxfordjournals.humrep.a019424.
65. Comai L. The advantages and disadvantages of being polyploid. Nat Rev Genet. 2005;6:836–46. doi:10.1038/nrg1711.
66. Ogden A, Rida PC, Knudsen BS, Kucuk O, Aneja R. Docetaxel-induced polyploidization may underlie chemoresistance and disease relapse. Cancer Lett. 2015;367:89–92. doi:10.1016/j.canlet.2015.06.025.
67. de Carne Trecesson S, Guillemin Y, Belanger A, Bernard AC, Preisser L, Ravon E, Gamelin E, Juin P, Barré B, Coqueret O. Escape from p21-mediated oncogene-induced senescence leads to cell dedifferentiation and dependence on anti-apoptotic Bcl-xL and MCL1 proteins. J Biol Chem. 2011;286:12825–38. doi:10.1074/jbc.M110.186437.
68. Liu M, Casimiro MC, Wang C, Shirley LA, Jiao X, Katiyar S, Ju X, Li Z, Yu Z, Zhou J, et al. p21CIP1 attenuates Ras- and c-Myc-dependent breast tumor epithelial mesenchymal transition and cancer stem cell-like gene expression in vivo. Proc Natl Acad Sci U S A. 2009;106:19035–9. doi:10.1073/pnas.0910009106.
69. Trail F. Fungal cannons: explosive spore discharge in the Ascomycota. FEMS Microbiol Lett. 2007;276:12–8. doi:10.1111/j.1574-6968.2007.00900.x.
70. Knop M. Yeast cell morphology and sexual reproduction–a short overview and some considerations. C R Biol. 2011;334:599–606. doi:10.1016/j.crvi.2011.05.007.